# Resonance-enhanced multiphoton ionization photoelectron spectroscopy of bound and autoionizing Rydberg states of atomic sulphur.

Woutersen, S.; Milan, J.B.; Buma, W.J.; de Lange, C.A.

**DOI**
10.1103/PhysRevA.54.5126

**Publication date**
1996

**Published in**
Physical Review A

# Resonance-enhanced multiphoton-ionization photoelectron spectroscopy of even-parity Rydberg states of atomic sulfur

S. Woutersen,* J. B. Milan, W. J. Buma, and C. A. de Lange
*Laboratory for Physical Chemistry, University of Amsterdam, Nieuwe Achtergracht 127, 1018 WS Amsterdam, The Netherlands*
(Received 17 June 1996; revised manuscript received 9 August 1996)

A (2+1) resonance-enhanced multiphoton-ionization photoelectron spectroscopy study of the sulfur atom was performed in the one-photon energy region between 260 and 240 nm. Some 20 previously unobserved even-parity Rydberg states of the sulfur atom are reported, which were accessed by two-photon transitions from the $^3P$ ground state of the atom, prepared by *in situ* photodissociation of $H_2S$. The $(^4S^o)np\ ^3P$ series could be followed up to $n=25$. This series is perturbed around $n=7$ by an interloping Rydberg state converging to the first excited ionic limit $^2D^o$. A two-channel quantum defect theory analysis was performed in order to estimate the composition of the wave functions of the perturbed series members, which is compared with the ionic state branching ratios obtained from photoelectron spectra. This analysis, moreover, enabled the determination of the ionization energy of the lowest ionic state $^4S^o$ with an improved accuracy as compared to the previously reported value. [S1050-2947(96)01612-5]

PACS number(s): 32.80.Rm

## I. INTRODUCTION

A detailed knowledge of the energy levels, oscillator strengths, and photoionization cross sections of the S atom is of fundamental interest for understanding the spectroscopy and dynamics of open-shell atoms [1] and is of astrophysical relevance because of the high abundance of sulfur in the interstellar medium and in the sun [2]. Previous studies have investigated both even- and odd-parity excited states of the atom. Vacuum ultraviolet absorption [3–5] and photoionization [6] studies have extensively covered transitions from the even-parity $^3P$ ground state of the atom to members of odd-parity Rydberg series converging upon both ground and excited states of the sulfur ion. Even-parity states of the atom have been investigated in several (2+1) resonance-enhanced multiphoton-ionization (REMPI) studies, in which atomic sulfur was produced by photolysis of $H_2S$ [7], $CS_2$ [8,9], $SO_2$ [10], and OCS [11]. These studies led to the assignment of many new even-parity Rydberg states, reached by two-photon excitation from either the ground or excited states of the atom.

Recently, we performed several (2+1) resonance-enhanced multiphoton-ionization photoelectron spectroscopy (REMPI-PES) studies of the mercapto (SH) radical in the wavelength region 258–208 nm [12–16]. The SH radicals were prepared by *in situ* photodissociation of $H_2S$. In these studies it was found that atomic sulfur was also produced, and a large number of two-photon transitions from both the $^3P$ ground and $^1D$ excited state of the atom were observed, reaching excited states both below and above the first ionization energy, many of which, to our best knowledge, have not yet been reported. The states above the first ionic limit will be discussed elsewhere [17]; here we will be concerned with the new states below the first ionic limit. These include high members ($n=9$–25) of the $(^4S^o)np\ ^3P$ Rydberg series. REMPI-PES was used to investigate in detail the composition of the electronic wave functions of these states. These studies revealed that the $(^4S^o)np\ ^3P$ Rydberg series is perturbed around $n=7$ by an interloping series converging to the $^2D^o$ excited ionic state. As a result ionic branching ratios are observed for ionization via these members which deviate considerably from those expected for unperturbed Rydberg states, i.e., ionization to a single ionic state which constitutes the ionic core of the Rydberg state.

## II. EXPERIMENT

The experimental setup has been described in detail previously [18]. In short, the frequency-doubled output of an excimer pumped dye laser (Lumonics HyperDye-500) is focused by a quartz lens with a focal length of 25 mm into a ''magnetic bottle'' spectrometer [19]. The spectrometer, which has primarily been designed for electron detection, has been modified to allow for mass-resolved ion detection as well. Excitation spectra were obtained by scanning the dye laser wavelength and monitoring the $S^+$ ion signal, the electron current, or an energy-selected part of the electron current. Photoelectron kinetic energy spectra were recorded by application of a variable retarding voltage on a grid surrounding the flight tube and transforming the high-resolution part of the time-of-flight spectrum. In this way a constant 10 meV resolution [full width at half maximum (FWHM)] at all kinetic energies can be achieved. Since the photoelectron acceptance angle is $2\pi$ sr, the relative intensities of the peaks in the photoelectron spectrum should exactly mirror the ionic state branching ratios.

The dye laser wavelength calibration was performed for the two-photon energy region 79 500–89 000 $cm^{-1}$, using the unambiguous assignment of 15 observed lines corresponding to two-photon transitions to known states of atomic sulfur and xenon. A least-squares fit was used to match literature values [20,21]. The rms deviation of the converted data from the literature values was found to be 0.3 $cm^{-1}$ at

*Present address: FOM-Institute for Atomic and Molecular Physics, Kruislaan 407, 1098 SJ Amsterdam, The Netherlands.

 

the two-photon level. The photoelectron energy scale was calibrated using (2+1) REMPI-PES via known excited states of sulfur.

Sulfur atoms were produced *in situ* by subsequent photodissociation of $H_2S$ and HS. Photodissociation of $H_2S$ results in a $^2S$ ground-state H atom together with a SH fragment in its ground vibronic level [22]. Photodissociation of SH leads to the formation of $H(^2S)$ and $S(^3P, ^1D)$, with a $S(^3P)$:$S(^1D)$ branching ratio of 3:1 [23]. The fine-structure branching ratio $S(^3P_2)$:$S(^3P_1)$:$S(^3P_0)$ has been found to be approximately statistical (5:3:1) [23].

In the present study, photodissociation and subsequent REMPI spectroscopy were carried out with one laser only. The concentration of sulfur atoms in the ionization chamber will therefore depend on the excitation wavelength, and caution must be exercised when interpreting intensity ratios in the observed spectrum. However, the S concentration is expected to vary slowly with the wavelength, allowing for a comparison of intensities of peaks lying within a short excitation energy interval.

$H_2S$ (99.6%, Messer Griesheim) was introduced into the ionization chamber using an effusive inlet. In order to avoid space-charge effects, the laser power was kept as low as possible, typically 1 mJ/pulse or less at the fundamental wavelength.

## III. RESULTS AND DISCUSSION

### A. General considerations

The ground-state electronic configuration of atomic sulfur is $1s^22s^22p^63s^23p^4$, which gives rise to the three terms $^3P$, $^1D$, and $^1S$ in order of increasing energy. The $^3P$ ground state is inverted, the $^3P_1$ and $^3P_0$ states lying 369.06 and 573.64 $cm^{-1}$ above the $^3P_2$ state, respectively; the energies of the $^1D_2$ and $^1S_0$ states are 9239.61 and 22 179.95 $cm^{-1}$ [20]. Removal of an outer electron produces the $S^+$ ion in its lowest electronic configuration, $\ldots 3p^3$, giving rise to the $^4S^o$ ground and $^2D^o$ and $^2P^o$ excited ionic states, which lie 83 559.1, 98 428 (mean value), and 108 107 $cm^{-1}$ (mean value) above the S I ground state, respectively [20].

In the present study two-photon transitions from the $^3P$ ground state are considered. Strict two-photon selection rules are $|\Delta J| = 0,1,2$ with $J=0 \leftrightarrow J=1$ forbidden, and the parity selection rule odd-odd, even-even. Because of the parity selection rule only transitions to the $(^4S^o)np$, $(^4S^o)nf$, $(^2D^o)np$, $(^2D^o)nf$, $(^2P^o)np$, and $(^2P^o)nf$ configurations, which have even parity, are allowed.

The states that are investigated in the present study are the $(^4S^o)np\ ^3P$ and $(^4S^o)nf\ ^3F$ Rydberg series. These states are best described in $LS$ coupling: since the $^4S^o_{3/2}$ ionic core has no spin-orbit splitting, the $LS$ approximation will hold up to high $n$ for $(^4S^o)nl$ states. In the $LS$ scheme the additional two-photon selection rules $\Delta S = 0$ and $|\Delta L| = 0,1,2$ (with $L=0 \leftrightarrow L=1$ forbidden) apply.

### B. Wavelength studies

Figure 1 shows part of the two-photon excitation spectrum of atomic sulfur measured in the present study, covering the two-photon energy region from 79 300 to 83 300 $cm^{-1}$. This spectrum was obtained employing mass-resolved ion detection and monitoring the $S^+$ channel. It was constructed by merging a number of shorter scans recorded under slightly different circumstances, which may cause discontinuities in the absolute intensities. Moreover, the spectrum was not corrected for the dye gain curve. The intensities of the peaks are therefore not quantitative, but the relative intensities of neighboring peaks within the same scan can be assumed to be reliable. Some of the resonances in the spectrum are caused by strong molecular REMPI processes showing up weakly in the $S^+$ channel. In Fig. 1 they are marked with asterisks.

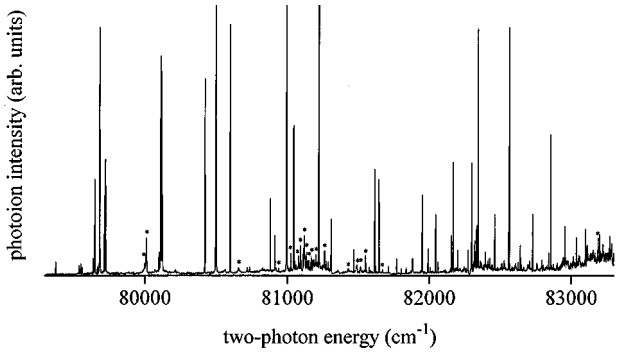


FIG. 1. Wavelength scan (not corrected for dye efficiency) covering the two-photon energy region from 79 300 to 83 300 $cm^{-1}$, recorded by monitoring the $S^+$ channel with mass-resolved ion detection. Peaks marked with asterisks are due to molecular resonances showing up in the $S^+$ channel.

The two-photon energy region 77 300–83 400 $cm^{-1}$, part of which is shown in Fig. 1, contains practically only transitions from the $^3P$ ground state to $(^4S^o)np$, $(^4S^o)nf$, and $(^2D^o)4p$ Rydberg states. Very few two-photon transitions from the $^1D_2$ excited state occur in this region; these transitions, which reach states above the first ionization energy, can be recognized by their photoelectron spectrum, and will be discussed elsewhere [17]. In this section the $(^4S^o)np$ and $(^4S^o)nf$ Rydberg states are considered. These were located by looking for the ground-state splittings $^3P_2$-$^3P_1$ and $^3P_2$-$^3P_0$ (396.1 and 573.6 $cm^{-1}$, respectively [20]) in the excitation spectrum. Occurrence of these splittings is conclusive evidence that the excited state is reached from the ground state. From the excitation energy relative to the $^3P_2$ ground state the quantum defect can be calculated, enabling identification of the orbital angular momentum $l$ of the Rydberg electron. When necessary, photoelectron spectra were recorded to identify the ionic core.

As was argued above, the Rydberg states converging to the $^4S^o$ limit are expected to be well described by $LS$ coupling. The fact that no transitions from the ground state to the $(^4S^o)np\ ^5P$ and $(^4S^o)nf\ ^5F$ quintet states were observed may be considered as an additional indication for the validity of the $LS$ approximation. The fine-structure splitting of the excited-state triplets could only be observed for the $(^4S^o)6p\ ^3P$ and $(^4S^o)7p\ ^3P$ states, both known from literature [20]; for $n>7$ the fine-structure splitting could no longer be resolved as a result of line broadening under the present experimental conditions (*vide infra*). In fact, even the $^3P_{0,1}$-$^3P_2$ splitting in $(^4S^o)8p\ ^3P$, determined previously as 0.43 $cm^{-1}$ [20], could not be resolved. As for the

TABLE I. Term values and quantum defects for the observed $(^4S^o)nf\ ^3F$ Rydberg states. Quantum defects have been calculated with respect to the energy of the $^4S^o$ ionic limit determined in the present work ($83\,560.8 \pm 0.1\ cm^{-1}$). Energy levels not previously observed are denoted by asterisks.

| Term values ($cm^{-1}$) | Assignment | $\mu$ |
|---|---|---|
| 80498.4 | $(^4S^o)6f\ ^3F$ | 0.014 |
| 81309.4 | $(^4S^o)7f\ ^3F$ | 0.018 |
| 81837.3 | $(^4S^o)8f\ ^3F$ | 0.021 |
| 82199.1* | $(^4S^o)9f\ ^3F$ | 0.023 |
| 82458.7* | $(^4S^o)10f\ ^3F$ | 0.021 |

$(^4S^o)nf\ ^3F$ states, resolution of the fine-structure splitting is not feasible, since it is less than 0.05 $cm^{-1}$ [20] even for the first member of the series.

With mass-resolved ion detection the $(^4S^o)nf\ ^3F$ series, which has previously been reported for $n=4$–8 [20], could be observed up to $n=10$. The observed energy levels and assignments are given in Table I. The $(^4S^o)np\ ^3P$ series, which has also been reported previously for $n=4$–8 [20], could be observed up to $n=17$ employing mass-resolved ion detection. For $n>17$ the resonant peak can no longer be distinguished from the background noise. However, when electron detection is employed, and only electrons with kinetic energies of $\sim 5$ eV are monitored, which derive from a (2+1) photoionization process of ground-state $^3P$ sulfur atoms to the $^4S^o$ ionic state, the $(^4S^o)np$ series can be observed up to $n=25$. Figure 2 shows the excitation spectrum using kinetic energy-selective electron detection, covering the two-photon energy range from 82 920 to 83 440 $cm^{-1}$, which embraces the $(^4S^o)np$ series from $n=15$ to $n=25$. The observed energy levels and assignments are given in Table II. For completeness the $(^2D^o)4p\ ^3P$ interloper state, which has been reported previously [20], is also included in this table. The energy values measured for the $(^4S^o)6p$ and $(^2D^o)4p$ states show a larger deviation from the literature values than would be expected (1.8 and 1.0 $cm^{-1}$, respectively [20]). This is due to the fact that our wavelength calibration was carried out only for the two-photon energy region from 79 500 to 89 000 $cm^{-1}$ and that extrapolation of this procedure may not be justified.

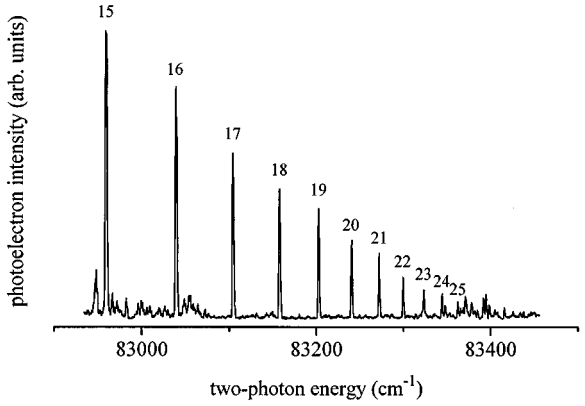


FIG. 2. Wavelength scan recorded by monitoring electrons with kinetic energies of $\sim 5$ eV, covering the two-photon region from 82 920 to 83 440 $cm^{-1}$. The small peaks which are not labeled correspond to molecular resonances.

TABLE II. Term values and quantum defects for the observed $(^4S^o)np\ ^3P$ Rydberg states. Quantum defects have been calculated with respect to the energy of the $^4S^o$ ionic limit determined in the present work ($83\,560.8 \pm 0.1\ cm^{-1}$). Energy levels not previously observed are denoted by asterisks.

| Term values ($cm^{-1}$) | Assignment | $\mu$ |
|---|---|---|
| 77892.1 | $(^4S^o)6p\ ^3P_2$ | 1.600 |
| 77904.1 | $(^4S^o)6p\ ^3P_0$ | 1.596 |
| 77915.5 | $(^4S^o)6p\ ^3P_1$ | 1.591 |
| 79376.3 | $(^2D^o)4p\ ^3P_2$ | 1.600[a] |
| 79406.3 | $(^2D^o)4p\ ^3P_1$ | 1.598[a] |
| 79419.0 | $(^2D^o)4p\ ^3P_0$ | 1.597[a] |
| 80112.8 | $(^4S^o)7p\ ^3P_2$ | 1.358 |
| 80120.5 | $(^4S^o)7p\ ^3P_1$ | 1.352 |
| 80123.8 | $(^4S^o)7p\ ^3P_0$ | 1.349 |
| 80995.8 | $(^4S^o)8p\ ^3P$ | 1.459 |
| 81619.0* | $(^4S^o)9p\ ^3P$ | 1.482 |
| 82044.6* | $(^4S^o)10p\ ^3P$ | 1.492 |
| 82344.8* | $(^4S^o)11p\ ^3P$ | 1.500 |
| 82564.9* | $(^4S^o)12p\ ^3P$ | 1.503 |
| 82730.0* | $(^4S^o)13p\ ^3P$ | 1.507 |
| 82857.7* | $(^4S^o)14p\ ^3P$ | 1.507 |
| 82958.9* | $(^4S^o)15p\ ^3P$ | 1.497 |
| 83038.6* | $(^4S^o)16p\ ^3P$ | 1.503 |
| 83103.6* | $(^4S^o)17p\ ^3P$ | 1.507 |
| 83157.4* | $(^4S^o)18p\ ^3P$ | 1.506 |
| 83202.3* | $(^4S^o)19p\ ^3P$ | 1.504 |
| 83239.9* | $(^4S^o)20p\ ^3P$ | 1.507 |
| 83271.9* | $(^4S^o)21p\ ^3P$ | 1.509 |
| 83299.3* | $(^4S^o)22p\ ^3P$ | 1.514 |
| 83323.3* | $(^4S^o)23p\ ^3P$ | 1.503 |
| 83344.0* | $(^4S^o)24p\ ^3P$ | 1.500 |
| 83362.0* | $(^4S^o)25p\ ^3P$ | 1.504 |

[a]Quantum defect calculated with respect to the $^2D^o$ ionic limit.

The resonances in Figs. 1 and 2 all have linewidths of 2.0 $cm^{-1}$ at the two-photon level, which is rather large, but can mainly be attributed to power broadening. When a lower laser intensity is employed, the linewidths can be reduced to 0.9 $cm^{-1}$. The laser bandwidth causes a broadening of 0.4 $cm^{-1}$. The velocity distribution of the S atoms will be virtually the same as the thermal distribution of the $H_2S$ molecules, as the two H atoms leaving the $H_2S$ molecule upon dissociation can hardly impart any momentum upon the remaining S atom. Under the assumption that the temperature of the latter distribution is about 300 K, the Doppler broadening is estimated to be 0.2 $cm^{-1}$ [24]. Therefore the observed line broadening can be accounted for.

Since the linewidths remain constant as $n$ increases, the peak heights for the two Rydberg series are expected to decrease as $(1/n^*)^3$, where $n^*$ is the effective quantum number. The experimentally observed drop in intensity is much more dramatic. For instance, from $n=22$ to $n=24$ the peak height reduces to half its value (see Fig. 2), whereas a factor of $\sim 0.77$ would be expected. A similar breakoff has been found to occur for the $np$ and $nf$ Rydberg series observed in

a REMPI-PES study of atomic nitrogen [25]. The breakoff cannot be due to field ionization, as fields of $\sim 800$ V/cm are needed to ionize $n=25$ states. Neither is it to be expected that the quadratic Zeeman effect resulting from the 1 T magnetic field would be responsible for the breakoff at these relatively low values of $n$ [26]. A more likely explanation would seem that the photoionization cross sections of the higher members become small enough that the photoionization step is no longer saturated at the laser fluence employed in this study. Using the method described in Ref. [27], the photoionization cross section was estimated to be $\sim 3\times 10^{-21}$ cm$^2$ for the $20p$ member, implying a saturation fluence of $\sim 300$ J cm$^{-2}$. Since the laser fluence used in our experiment is at most about 1000 J cm$^{-2}$, the ionization step will not be saturated for the $n>20$ members. Because the ionization cross section decreases as $(1/n^*)^3$, the line strengths in the series will then show a transition from a $(1/n^*)^3$ to a $(1/n^*)^6$ proportionality as $n$ increases.

### C. Two-channel quantum defect theory analysis of the perturbed $(^4S^o)np\ ^3P$ Rydberg series

The $(^4S^o)np\ ^3P$ Rydberg series is strongly perturbed around the $n=7$ member by the $(^2D^o)4p\ ^3P$ interloper state. This perturbation manifests itself clearly in the observed quantum defects (cf. Table II). The $(^2D^o)4p\ ^3P$ state is the only even-parity $^3P$ state below the first ionization energy (IE) that converges to an excited ionic limit. The $(^2D^o)5p\ ^3P$ and $(^2P^o)4p\ ^3P$ states have not been observed yet, but are expected to lie well above the first IE. It appears that in a rough analysis only the $(^2D^o)4p\ ^3P$ state has to be considered in order to account for the perturbation in the $(^4S^o)np\ ^3P$ Rydberg series. In first approximation, states other than $^3P$ do not have to be included, since $L$ and $S$ are approximately good quantum numbers. Furthermore, since $J$ is a good quantum number, $(^4S^o)np\ ^3P_0$ will only interact with $(^2D^o)4p\ ^3P_0$, $(^4S^o)np\ ^3P_1$ only with $(^2D^o)4p\ ^3P_1$, and $(^4S^o)np\ ^3P_2$ only with $(^2D^o)4p\ ^3P_2$. Hence the problem reduces to three two-channel problems.

Accordingly, three two-channel quantum defect theory (QDT) analyses (for $^3P_0$, $^3P_1$, and $^3P_2$) have been performed to assess the degree of mixing, and hence the relative contributions of the $(^4S^o)np$ and $(^2D^o)4p$ configurations in the wave functions. Writing the wave functions as

$$\Psi(^3P_J)=c_1\psi[(^4S^o)np\ ^3P_J]+c_2\psi[(^2D^o)4p\ ^3P_J], \quad (1)$$

for $J=0,1,2$, the mixing ratio $c_1/c_2$ can be calculated for every $n$, provided the 2QDT parameters are known, viz., the two eigen quantum defects $\mu_1$ and $\mu_2$ and a third parameter describing the $2\times 2$ unitary matrix $U_{i\alpha}$ [28]. These quantities were found by performing a least-squares-fitting procedure using the measured term levels. The least-squares procedure requires that the theoretical term levels be calculated for a given set of parameters $\{\mu_i, U_{i\alpha}\}$. Since the calculation gives only the effective quantum number $n^*$ modulo 1, the integral part was supplied by the experimental term levels. The uncertainty was supposed to be equal for all the measured term values (note that in that case the uncertainty in the effective quantum numbers $n^*$ will be proportional to $n^{*3}$).

TABLE III. $^4S^o$ ionization energy and 2QDT parameters for the $(^4S^o)np\ ^3P_2$ series obtained by least-squares fitting. The numbers in parentheses correspond to the standard deviation in the last significant digits.

| | |
|---|---|
| $I(^4S^o)$ (cm$^{-1}$) | 83560.8(1) |
| $\mu_1$ | 0.4714(2) |
| $\mu_2$ | 0.6446(2) |
| $U_{11}$ | 0.8147(9) |
| $U_{12}$ | −0.579(1) |
| rms deviation (cm$^{-1}$) | 0.32 |

For the analyses the observed term levels of the Rydberg states from $n=7$ to $n=25$ were used. The lower levels from $n=4$ to $n=6$ were excluded as their energies are expected to be affected by polarization of the ionic core by the outer electron [28]. Furthermore, an infrared emission study of atomic sulfur has shown evidence for substantial configuration interaction between the $(^4S^o)6p\ ^3P_1$ and the $(^4S^o)6p\ ^5P_1$ and $(^2D^o)4p\ ^1P_1$ states [29]. In fact, preliminary fits, in which the $(^4S^o)6p\ ^3P$ state was included, gave rise to considerably larger rms deviations, thereby showing that the term energy of this state is perturbed by other factors than only interaction with the $(^2D^o)4p\ ^3P$ levels. For the term level of the $(^2D^o)4p$ state the literature value was used because of the relatively large error observed for this level in our study (see Sec. III B).

Since the fine-structure splitting could only be resolved for the $(^4S^o)7p\ ^3P$ state, carrying out separate analyses for every value of $J$ is a somewhat artificial procedure. As may be expected, the results are virtually independent of $J$. The results of the fit are given in Table III, while in Fig. 3 the corresponding Lu-Fano plot is shown. From this analysis an improved value of the ionization energy of the $^4S^o$ ionic state is derived as $83\,560.8\pm 0.1$ cm$^{-1}$. Before the present study the $^4S^o$ ionization energy was only known with an accuracy of 1.0 cm$^{-1}$, mainly because it had been determined from the excitation energies of a limited number of the $(^4S^o)nl$ Rydberg states with $n$ limited to values smaller than 11. Using the parameters given in Table III the mixing coefficients of the $(^4S^o)np\ ^3P_2$ and $(^2D^o)4p\ ^3P_2$ levels can be calculated. They are given for the first members in Table IV, together with the calculated term values. The interloper state is also included in this table.

### D. Photoelectron study of the $(^4S^o)np\ ^3P$ Rydberg series

Photoelectron spectra have been obtained following two-photon resonant, three-photon ionization via the members $n=6$–15 and $n=20$ of the $(^4S^o)np\ ^3P$ Rydberg series and via the $(^2D^o)4p\ ^3P_2$ interloper state. The $(2+1)$ ionization process always took place from the $^3P_2$ ground state. In all cases the three-photon energy exceeded the third ionization limit, allowing photoionization into the $^4S^o$, $^2D^o$, and $^2P^o$ continua. The $^2D^o$ and $^2P^o$ fine-structure splittings (4 and 6 meV, respectively) could not be resolved, since the best achievable energy resolution was 10 meV. Figures 4(a)–4(f) show some representative photoelectron spectra, and the observed ionic state branching ratios are given in Table V. The values for the $6p$ level agree well with those reported in a previous REMPI-PES study of atomic sulfur [10].

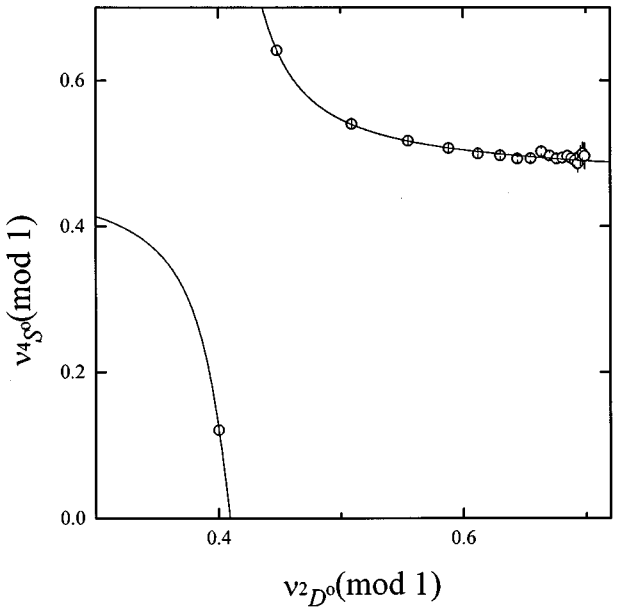


FIG. 3. Lu-Fano plot of the perturbed $(^4S^o)np\ ^3P_2$ Rydberg series. The solid line results from a least-squares fitting of the term values of the $n=7$ to $n=25$ members (see the text for details).

Ionization to the $^2P^o$ excited ionic state is seen to be very weak, the corresponding branching ratios being typically less than 5%. It seems unlikely that this nonzero $^2P^o$ branching value is due to configuration interaction at the two-photon level, as there are no $(^2P^o)np$ or $(^2P^o)nf$ states in the energy region below 87 000 $cm^{-1}$. However, the $^2P^o$ photoionization matrix element might be much larger than the $^4S^o$ photoionization matrix element, rendering even a slight amount of mixing of $(^2P^o)np$ or $(^2P^o)nf$ states observable in the photoelectron spectrum. Although this possibility cannot be ruled out, it seems more probable that the nonzero $^2P^o$ branching ratio is due to configuration interaction in the ionization continuum.

The branching ratios to the $^2D^o$ ionic state are expected to follow roughly the compositions of the Rydberg state wave functions which were calculated above (cf. Table IV). However, a direct quantitative comparison between the branching ratios observed in the photoelectron spectra and the wave function composition is not straightforward, since the relative photoelectron intensities will depend on the

TABLE IV. Calculated and observed term values and relative contributions $|c_1|^2$ and $|c_2|^2$ to the wave function $\Psi$ as given in Eq. (1). Only the values for the $(^4S^o)np\ ^3P_2$ series and for $(^2D^o)4p\ ^3P_2$ are given.

| State | Calculated term value ($cm^{-1}$) | Observed term value ($cm^{-1}$) | $\lvert c_1\rvert^2$ (%) | $\lvert c_2\rvert^2$(%) |
|---|---|---|---|---|
| $(^4S^o)6p$ | 77908.0[a] | 77890.5[ab] | 91 | 9 |
| $(^2D^o)4p$ | 79375.8 | 79375.8[b] | 45 | 55 |
| $(^4S^o)7p$ | 80112.9 | 80112.8 | 76 | 24 |
| $(^4S^o)8p$ | 80995.3 | 80995.8 | 96 | 4 |
| $(^4S^o)9p$ | 81618.9 | 81619.0 | 99 | 1 |
| $(^4S^o)10p$ | 82044.7 | 82044.6 | 99 | 1 |
| $(^4S^o)11p$ | 82345.5 | 82344.8 | 100 | 0 |
| $(^4S^o)12p$ | 82565.3 | 82564.9 | 100 | 0 |
| ⋮ | ⋮ | ⋮ | ⋮ | ⋮ |

[a]This term value was not used in the fit.

[b]These values were taken from literature [20].

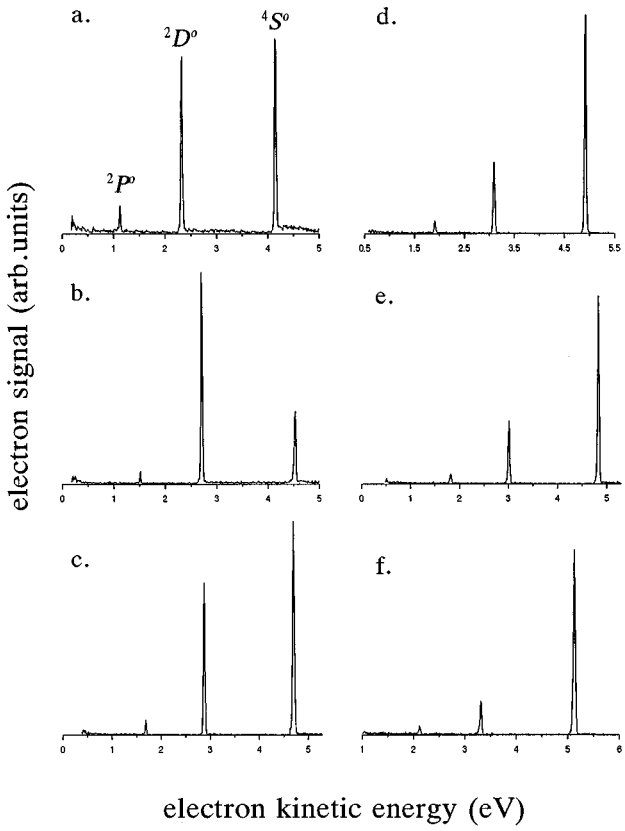


FIG. 4. Photoelectron spectra obtained following ionization from the $^3P_2$ ground state via the $n=6$ (a), $n=7$ (b), $n=8$ (c), $n=9$ (d), $n=10$ (e), $n=15$ (f) members of the $(^4S^o)np\ ^3P$ Rydberg series.

TABLE V. Observed ionic state branching ratios for the $(^4S^o)np\ ^3P$ Rydberg series and the $(^2D^o)4p\ ^3P_2$ interloper.

| Resonant state | $^2P^o$ (%) | $^2D^o$ (%) | $^4S^o$ (%) |
|---|---|---|---|
| $(^4S^o)6p\ ^3P_2$ | 6 | 41 | 54 |
| $(^4S^o)6p\ ^3P_0$ | 4 | 26 | 70 |
| $(^4S^o)6p\ ^3P_1$ | 11 | 44 | 45 |
| $(^2D^o)4p\ ^3P_2$ | 2 | 82 | 16 |
| $(^4S^o)7p\ ^3P_2$ | 2 | 67 | 30 |
| $(^4S^o)7p\ ^3P_1$ | 2 | 68 | 30 |
| $(^4S^o)7p\ ^3P_0$ | 2 | 68 | 30 |
| $(^4S^o)8p\ ^3P$ | 3 | 36 | 61 |
| $(^4S^o)9p\ ^3P$ | 4 | 25 | 71 |
| $(^4S^o)10p\ ^3P$ | 3 | 22 | 75 |
| $(^4S^o)11p\ ^3P$ | 4 | 16 | 80 |
| $(^4S^o)12p\ ^3P$ | 5 | 13 | 81 |
| $(^4S^o)13p\ ^3P$ | 4 | 18 | 79 |
| $(^4S^o)14p\ ^3P$ | 3 | 15 | 82 |
| $(^4S^o)15p\ ^3P$ | 3 | 14 | 83 |
| $(^4S^o)20p\ ^3P$ | 3 | 13 | 84 |

$(^4S^o)np$ and $(^2D^o)4p$ photoionization matrix elements. Writing the wave functions as Eq. (1), the relative ionic state branching ratios are given by

$$|\langle\psi^+[(^4S^o)\epsilon l]|\vec{\mu}|c_1\psi[(^4S^o)np]+c_2\psi[(^2D^o)4p]\rangle|^2 \quad (2)$$

and

$$|\langle\psi^+[(^2D^o)\epsilon l]|\vec{\mu}|c_1\psi[(^4S^o)np]+c_2\psi[(^2D^o)4p]\rangle|^2, \quad (3)$$

where $\psi^+$ denotes the wave function of the final ion-continuum system. Since $\vec{\mu}$ is a one-electron operator, the branching ratios (2) and (3) reduce to

$$|c_1|^2|\langle\psi^+[(^4S^o)\epsilon l]|\vec{\mu}|\psi[(^4S^o)np]\rangle|^2 \quad (4)$$

and

$$|c_2|^2|\langle\psi^+[(^2D^o)\epsilon l]|\vec{\mu}|\psi[(^2D^o)4p]\rangle|^2. \quad (5)$$

Therefore the relative branching ratios are determined by the ratio $|c_1/c_2|^2$ as well as the magnitude of the photoionization matrix elements. This should be kept in mind when discussing photoelectron peak intensities. As can be seen in Table V and Figs. 4(a)–4(f), these peak intensities roughly track the wave function composition, the $^2D^o$ peak intensity reaching a maximum for the $(^4S^o)7p\ ^3P$ level [Fig. 4(b)], which interacts most strongly with the $(^2D^o)4p\ ^3P$ interloper, and then decreasing slowly as $n$ increases [Figs. 4(c)–4(f)]. Comparison of the observed branching ratios (Table V) with the squared coefficients $|c_1|^2$ and $|c_2|^2$ (Table IV) shows that ionization to the $^2D^o$ ionic state is strongly enhanced for all Rydberg wave functions having both $(^4S^o)np$ and $(^2D^o)4p$ character. In fact, even for the virtually unperturbed $(^4S^o)15p\ ^3P$ level, the transition to the $^2D^o$ ionic state is still appreciable [Fig. 4(f)].

For REMPI via the $(^4S^o)6p\ ^3P_J$ state the ionic branching ratios show an interesting $J$ dependence (cf. Table V), ionization via the $^3P_1$ and $^3P_2$ components yielding significantly more $^2D^o$ ions than ionization via the $^3P_0$ component. A $J$ dependence of the photoionization matrix element would seem unlikely, since in that case a similar effect would be expected for the $7p\ ^3P_J$ state. The effect may be due to configuration interaction with $(^2D^o)4p$ singlet levels. The evidence from IR spectroscopy for mixing of the $(^4S^o)6p\ ^3P_1$ and $(^2D^o)4p\ ^1P_1$ states has already been mentioned. In a previous REMPI study of atomic sulfur [9] observed singlet-triplet transitions were attributed to the effects of configuration interaction between the $(^4S^o)6p\ ^3P_2$ and $(^2D^o)4p\ ^1D_2$ states. As the $(^4D^o)4p$ configuration does not give rise to a singlet state with $J=0$, such an interaction cannot occur for the $(^4S^o)6p\ ^3P_0$ level and a lower $^2D^o$ branching ratio might consequently be expected for ionization via this state.

## IV. CONCLUSIONS

In summary, some 20 previously unobserved even-parity Rydberg states of the sulfur atom converging to the lowest ionization threshold are reported and assigned. The states were accessed by two-photon excitation from the $^3P$ ground state. REMPI-PES was employed to determine the ionic state branching ratios upon photoionization of these states. The $(^4S^o)np\ ^3P$ series converging to the ionic ground state was followed up to $n=25$. The extensive observation of this series allowed for a more accurate determination of the lowest ionization energy as $83\,560.8\pm0.1\ \mathrm{cm}^{-1}$. The perturbation of the series by the $(^2D^o)4p\ ^3P$ interloper state was observed in the ionic state branching ratios of the $(^4S^o)np\ ^3P$ states.

## ACKNOWLEDGMENTS

The authors gratefully acknowledge the Netherlands Organization for Scientific Research (NWO) for financial support. We thank J. H. Hoogenraad and L. D. Noordam for helpful discussions.

[1] Z. Altun, J. Phys. B **25**, 2279 (1992).
[2] R. P. Wayne, J. Photochem. Photobiol. A-Chem. **62**, 379 (1992).
[3] G. Tondello, Astrophys. J. **172**, 771 (1972).
[4] V. N. Sarma and Y. N. Joshi, Physica C **123**, 349 (1984).
[5] Y. N. Joshi, M. Mazzoni, A. Nenecioni, W. H. Parkinson, and A. Cantu, J. Phys. B **20**, 1203 (1987).
[6] S. T. Gibson, J. P. Greene, B. Ruscić, and J. Berkowitz, J. Phys. B **19**, 2825 (1986).
[7] J. Steadman and T. Baer, J. Chem. Phys. **89**, 5507 (1988).
[8] P. Brewer, N. van Veen, and R. Bersohn, Chem. Phys. Lett. **91**, 126 (1982).
[9] T. V. Ventikachalam and A. S. Rao, Appl. Phys. B **52**, 102 (1991).
[10] J. R. Appling, M. R. Harbol, and R. A. Edgington, J. Chem. Phys. **97**, 4041 (1992).
[11] S. T. Pratt, Phys. Rev. A **38**, 1270 (1988).
[12] J. B. Milan, W. J. Buma, C. A. de Lange, K. Wang, and V. McKoy, J. Chem. Phys. **103**, 3262 (1995).
[13] J. B. Milan, W. J. Buma, C. A. de Lange, C. M. Western, and M. N. R. Ashfold, Chem. Phys. Lett. **239**, 326 (1995).
[14] J. B. Milan, W. J. Buma, and C. A. de Lange, J. Chem. Phys. **104**, 521 (1996).
[15] J. B. Milan, W. J. Buma, and C. A. de Lange, J. Chem. Phys. **105**, 6688 (1996).
[16] J. B. Milan, W. J. Buma, C. A. de Lange, K. Wang, and V. McKoy (unpublished).
[17] S. Woutersen, J. B. Milan, W. J. Buma, and C. A. de Lange (unpublished).
[18] M. R. Dobber, W. J. Buma, and C. A. de Lange, J. Chem. Phys. **101**, 9303 (1994).
[19] P. Kruit and F. H. Read, J. Phys. E **16**, 313 (1983).
[20] W. C. Martin, R. Zalubas, and A. Musgrove, J. Phys. Chem. Ref. Data **19**, 820 (1990).
[21] C. E. Moore, in *Atomic Energy Levels*, Vol. 3 of Natl. Stand. Ref. Data Ser., Natl. Bur. Stand. (U.S.) No. 35 (U.S. GPO, Washington, DC, 1971).

[22] G. P. Morley, I. R. Lambert, D. H. Mordaunt, S. H. S. Wilson, M. N. R. Ashfold, R. N. Dixon, and C. M. Western, J. Chem. Soc. Faraday Trans. **89**, 3865 (1993).
[23] C.-W. Hsu, C.-L. Liao, Z.-X. Ma, P. J. H. Tjossem, and C. Y. Ng, Chem. Phys. Lett. **199**, 78 (1992).
[24] I. Sobelman, *Atomic Spectra and Radiative Transitions* (Springer-Verlag, New York, 1979).
[25] E. de Beer, C. A. de Lange, and N. P. C. Westwood, Phys. Rev. A **46**, 5653 (1992).
[26] L. D. Noordam, M. P. de Boer, and H. B. van Linden van den Heuvell, Phys. Rev. A **41**, 6267 (1990).
[27] H. G. Muller, Ph.D. thesis, Free University, Amsterdam, 1985.
[28] J. J. Wynne and J. A. Armstrong, Phys. Rev. A **15**, 180 (1977).
[29] L. R. Jakobsson, Ark. Fys. **34**, 19 (1967).